Efficient biogenesis of Au nanoparticles using extract of Mentha pulegium flower: Evaluation of catalytic reduction of nitroarenes and anti-human colon cancer properties in the in vitro condition

Shabnam Bovandi

Payame Noor University Department of Chemistry

Maryam Shahriari

Islamic Azad University

Mohammad Mahdi Zangeneh (✉ m.mehdizangeneh@yahoo.com)

Ilam University of Medical Sciences

Abstract

Background

With regards to applicative, facile, green chemical research, a bio-inspired approach is being reported for the synthesis of Au nanoparticles by using *Mentha pulegium* flower extract.

Methods

The phytochemical immobilized Au NPs were characterized by advanced physicochemical techniques like Fourier Transformed Infrared spectroscopy (FT-IR), Scanning Electron Microscopy (SEM), Transmission Electron Microscopy (TEM), Energy Dispersive X-ray spectroscopy (EDX), and X-ray Diffraction (XRD) study. Thereafter, catalytic performance of those biomolecule functionalized Au NPs was investigated in the efficient reduction of nitroarenes over a range of substrates. To survey the anti-human colon cancer effects of gold nanoparticles, MTT assay was used on the common colon cancer cell lines i.e., colorectal adenocarcinoma (HT-29), colorectal carcinoma (HCT 116), ileocecal colorectal adenocarcinoma (HCT-8 [HRT-18]), and Burkitt's lymphoma (Ramos.2G6.4C10).

Results

The conversion was achieved in short reaction time with good to excellent yields in association with outstanding turnover frequency (TOF). In addition, the nanocomposite catalyst was easily recovered and recycled for 12 successive times without noticeable decrease in catalytic activity. Gold nanoparticles had high anti-colon cancer activities dose-dependently against HT-29, HCT 116, HCT-8 [HRT-18], and Ramos.2G6.4C10 cell lines. The best result of anti-colon cancer effects was seen in the case of the HCT 116 cell line.

Conclusions

It looks gold nanoparticles can be used for the treatment of several types of colon cancers in human.

Introduction

In the last few decades' nanotechnology has been considered as one of the most emerging field in science. The technology has emerged extremely promising based on its extensive applications in different fields like engineering, physics, biology and chemistry and their interdisciplinary arena [1−4]. More specifically, nanosciences have been exploited in regions like drug delivery targeting cancer cell and other deadly ailments [5], water purifications [6], electronics [7], imaging contrast agents [8] and catalysis [9−12]. We are particularly interested in nanocatalysis as the corresponding materials are having unique criteria like extremely small dimension, high surface to volume ratio, exceptional shape dependant

properties, uniformity in particle size distribution, truly heterogeneous nature and reusable with almost constant efficiency [13–16]. They satisfy almost all the criteria as for an ideal catalyst.

Green chemistry offers a cohesive set of twelve principles and has engrossed widespread interest in view of sustainability [17]. One of the most important future perspectives of green chemistry is designing ecological or bio-inspired catalysts in pursuing important organic transformations. The concept of greener nanoscience is a practical approach towards advanced applications of nanotechnology [18–21].

Following this coalescence between nanotechnology and green chemistry, the biogenic synthesis of NPs has evolved as an outstanding progress in the design of eco-friendly catalysts. Extract of different parts of plants like fruits, barks, flowers, roots leaves etc contain several phytochemicals like polyphenols, flavonoids, alkaloids, mild acids and terpenoids which have been found to be very effective in the biometric conversion of metal salts into corresponding NPs [22–27]. In the recent past, this green metric protocol for the synthesis of noble metal NPs has been quite popular [28–31] and ample studies are going on for the biogenic synthesis of Au nanoparticles [32–37]. Au NPs find extensive applications in diverse fields like biological transmission electron microscopy, colorimetric DNA sensors based on colloidal Au and catalysis [38]. As being a catalyst, Au NP displays considerable potential towards various organic transformations [39–42]. This actually has prompted us to carry out the biogenic green synthesis of Au NP and exploring its catalytic performance in the efficient reduction of different nitroarenes.

Reduction of nitroarenes is one of the elementary but significant organic reactions having outstanding implications. The as synthesized aromatic amines are relatively safer chemical and have wide range of synthetic and biological applications like photographic development, corrosion inhibition, anticorrosion lubrication and in pharmaceuticals for the preparation of analgesic, antipyretic and other drugs [43–45]. The nitrophenols derivatives are known to be significant organopollutant of water and being produced from herbicides, pesticides and synthetic dyes. They are highly toxic for animals and humans and cause disorderness of liver, kidney and central nervous system. Reductions of nitrophenols generate the safer and non-toxic aminophenols which has several other applications [46–47].

The *Mentha pulegium* plant has a high ornamental and medicinal importance and value, and attracts lots of tourists worldwide for seeing the Crown Imperial in the wild. In Iran, *Mentha pulegium* wild populations are at risk of fast eradication, due to irregular grazing of *Mentha pulegium* stands, deficiency in protecting rules, pest overflow, and altering the pastures to dry farmlands [48]. The bulbs of various *Mentha pulegium* species have been applied as a crucial anti-hypertensive drug and anti-tussive, expectorant in traditional chinese medicine [49]. The main constituents of this plant include polyphenols, alkaloids, organic acids, terpenoids, carbohydates and *etc*. [50]. Now, based on the research on the biosynthesis of metal NPs and heterogeneous catalysis [51–55], we report herein the green synthesis of Au NPs using *Mentha pulegium* flower extract for the first time and investigated its catalytic performance in the reduction of nitroarenes using $NaBH_4$ as the hydride source (Scheme 1). The flower is grown widely in Himalaya plateau and rich in important phytochemicals. Our protocol showed excellent catalytic

reactivity over a wide spectrum of nitroarenes in water. Also, we decided to investigate the anti-colon cancer potentials of gold nanoparticles formulated by *Mentha pulegium* flower against colorectal adenocarcinoma, colorectal carcinoma, ileocecal colorectal adenocarcinoma, and Burkitt's lymphoma cell lines.

2. Experimental

2.1. Preparation of *Mentha pulegium* flower extract

Fresh *Mentha pulegium* flowers were collected and washed thoroughly with double-distilled water. 2.0 g of the flower petals was boiled in 100 mL deionized water for 20 min. The colored mixture was then cooled and filtered through Whatmann filter paper No. 1 to have the aqueous extract. It was stored at 4 °C in refrigerator for further use.

2.2. Green synthesis of Au NPs using *Mentha pulegium* flower extract

In a 50 mL 1 (mM) aqueous solution of $HAuCl_4$ 10 mL of the flower extract was added in stirring condition at room temperature. After 20 min, the light yellow colored mixture changed to wine red, an indication for the synthesis of Au NPs (Fig. 2). Then the solution containing nanoparticles was centrifuged at 4000 rpm for 20 min and the upper transparent layer was decanted off. The residues obtained were washed for several times with deionized water and finally dried in an oven at 50°C.

2.3. Reduction of nitrobenzene to aniline

In the typical procedure, 2 mg (0.1 mol%) of the synthesized Au NPs was added to a solution of nitrobenzene (1 mmol) in H_2O/MeOH (2:1, 3 mL) mixture and was stirred for 5 min. Then, $NaBH_4$ solution (2 mmol) was added and the reaction mixture was heated to 60 °C. Progress of the reaction was monitored by thin layer chromatographic (TLC) [n-hexane/EtOAc : 4/1] and after completion, the mixture was diluted with EtOAc. The catalyst was isolated by centrifugation, washed and dried separately for reuse. The total organic layer containing the product was dried over anhydrous Na_2SO_4 and concentrated to have pure aniline.

2.4 Measurement of the anti-human colon cancer effects of Au NPs

In this experiment, the following cell lines have been used for investigating the anti-human colon cancer effects of the $HAuCl_4$, *Fritillaria Imperialis* flower, and Au NPs using an MTT assay:

1) Colorectal adenocarcinoma: HT-29.

2) Colorectal carcinoma: HCT 116.

3) Ileocecal colorectal adenocarcinoma: HCT-8 [HRT-18].

4) Burkitt's lymphoma: Ramos.2G6.4C10.

For culturing the above cells, penicillin, streptomycin, and Dulbecco's modified Eagle's medium (DMEM) were used. The distribution of cells was 10,000 cells/well in 96-well plates. Then, all samples were transferred to a humidified incubator with 5% CO_2 at the temperature of 37 °C. After 24 h incubating, all cells were treated with several concentrations of $HAuCl_4$, *Fritillaria Imperialis* flower, and Au NPs, then incubated for 24 h. $HAuCl_4$, *Fritillaria Imperialis* flower, and Au NPs were sterilized using the radiation of UV for 2 h. Finally, 5 mg/mL of MTT was added to all wells and all samples were transfer to an incubator at the temperature of 37 °C for 4 h. The percentage of cell viability of samples was measured at the absorbance of 570 nm and according to the following formula [53].

Percentage of cell viability (%) = (Sample absorbance/Control absorbance) × 100

3. Results And Discussion

3.1. Characterizations of biosynthesized Au NPs

Biogenic reduction of Au^{3+} ions to Au NPs over the plant extract could be monitored visibly by color change and spectroscopically by UV-Vis technique. The instant the *Mentha pulegium* extract was added into the aqueous solution of $HAuCl_4$, color of the solution started changing from yellow to dark red (Fig. 1). Surface Plasmon resonance phenomenon confirmed the formation of Au NPs. As the reaction progressed, intensity of the color increased. In addition to visible tracking, a UV-Vis spectrum of the reaction solution was also recorded to detect the progression of the reaction. Fig. 1 displays the characteristic change as the initial peak due to Au(III) at ~520 nm disappeared as the reaction went to completion to Au (0).

The as synthesized Au NPs were characterized with analytical techniques like Fourier Transformed Infrared Spectroscopy (FT-IR), Scanning Electron Microscopy (SEM), Transmission Electron Microscopy (TEM), Energy Dispersive X-ray spectroscopy (EDX) and Powder X-ray diffraction (XRD).

Fig. 2 represents the FT-IR spectra of *Mentha pulegium* extract itself (a) and the biomolecule modified Au NPs (b). The extract shows strong signals at 3402 cm^{-1}, 2872 cm^{-1} and 1679 cm^{-1} which are attributed to phenolic O-H, C-H and C=O bonds respectively. The FT-IR profile of the flower extract almost overlaps with the Au NP spectrum. This clearly indicates the successful immobilization of flower phytochemicals over Au NPs. The results obtained from the FT-IR spectra confirmed that nanoparticles are coated with biomolecules, especially with the amino acid residues of the proteins. The amino acid residues of proteins have a strong ability to bind with metal by coating their surface and preventing them from aggregation and are responsible for reduction and stabilizing. Thus, from the above discussion, it can be concluded that biomass (protein, phenolic, and alcoholic compounds) perform the function of stabilizing and reducing agents for Au NPs [15].

Structural morphology of the biosynthesized Au NPs was investigated by SEM and HR-TEM techniqes. The SEM image, presented in Fig. 3, depicts lump like agglomerations which might be due to high concentration during sampling. However, in a closer view it shows polyhedron and spherical globules adhered homogeneously. Due to tiny size the particles have high tendency towards association. The HR-TEM images display a better structural insight with a clear view of the particle shape and size of Au NPs. As can be seen from Fig. 4, most of the nanoparticles are of homogeneous pherical and octahedral shapes. Average diameter of the particles are within 30-45 nm. Such shape variance could be explained based on Ostwald ripening theory where a large number of small active particles are associated resulting in the growth of larger nanoparticles of anonymous shape and size [32]. There is an agreement between the SEM image and HR-TEM images of the biosynthesized Au NPs.

Energy Dispersive X-ray Spectroscopy (EDX) confirmed the existence of pure Au particles in the specimen (Fig. 5). The presence of C and O elements justifies the phytochemical functionalizations over Au NPs. As the sample preparation was done on a Cu grid, it appears in the profile by default.

In order to investigate the crystalline nature of Au NPs, XRD analysis was performed. As shown in Fig. 6, the characteristic peak position, width and height in the pattern resembles the face centered cubic (*fcc*) gold. The standard cubic phase of gold, (JCPDS No.65-2870) contains (1 1 1), (2 0 0), (2 2 0) and (3 1 1) planes at 2θ values of 38.2, 44.55, 63.85 and 76.85 respectively which is found to be in close agreement with our material. The other small insignificant peaks can be attributed to phytochemicals present in the flower extract.

3.2. Catalytic performance of the biogenic Au NPs

Following the meticulous physicochemical characterizations of the biosynthesized catalyst, it was the turn to explore its catalytic activity. We investigated the catalyst in the reduction of nitroarenes using $NaBH_4$ as hydride source. At the outset, optimization of reaction conditions was intended and thereby different reaction conditions like catalyst load, solvent and temperature were assorted over a probe reaction, the reduction of nitrobenzene. The experimental outcomes are shown in table 1. The reaction was failed in the absence of any catalyst which signifies alone $NaBH_4$ is not sufficient to carry out the nitro reduction (entry 1, Table 1). 2.0 mmol $NaBH_4$ was required for complete reduction in presence of the catalyst. While studying the solvent effect over the model reaction, the best result was achieved in $MeOH/H_2O$ mixture (2 : 1) among the different tested solvents like EtOH, MeOH, H_2O, DMF and CH_3CN. (entries 2-6, Table 1). 0.1 mol% of catalyst load was found to produce the best result (entry 8, table 1). Again, keeping the other conditions intact, it was observed that the reaction worked the best at 60 °C.

Table 1. Optimization of the reduction of nitrobenzene with $NaBH_4$ in the presence of Au NPs under various conditions.[a]
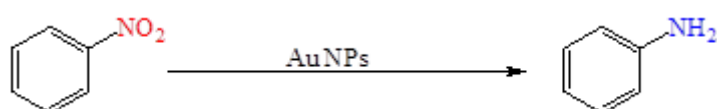
Entry	Au (mol%)	Solvent	NaBH$_4$ (mmol)	T (°C)	Time (h)	Yield (%)[b]
1	-	EtOH	2	60	24	0
2	0.1	EtOH	2	60	1	60
3	0.1	MeOH	2	60	1	70
4	0.1	H$_2$O	2	60	2	50
5	0.1	DMF	2	60	1	55
6	0.1	CH$_3$CN	2	60	1	40
7	0.1	H$_2$O-MeOH (1:1)	2	60	1	80
8	0.1	H$_2$O-MeOH (2:1)	2	60	1	98
9	0.05	H$_2$O-MeOH (2:1)	2	60	1	80
10	0.1	H$_2$O-MeOH (2:1)	1.5	60	1	88
11	0.1	H$_2$O-MeOH (2:1)	2.5	60	1	98
12	0.1	H$_2$O-MeOH (2:1)	2	50	2	88
13	0.1	H$_2$O-MeOH (2:1)	2	25	2	50
14	0.1	H$_2$O-MeOH (2:1)	2	70	1	98

[a]Reaction conditions: nitrobenzene (1.0 mmol), solvent (3.0 mL), open air; [b]Isolated yield.

After having the standard conditions in hand for the reduction of nitro compounds, it was the turn to establish the scope and generality of those conditions. Diverse ranges of nitroarenes were reduced to corresponding amines in presence of the Au NP over NaBH$_4$. The results have been depicted in Table 2. Both electron attracting and electron withdrawing groups are found to be equally compatible under the reaction conditions producing excellent yields within 1-2 h time range. Turnover frequencies (TOF) are being calculated in all the cases which are moderate to high as presented in table 2.

Table 2. Au NPs catalyzed reduction of aromatic nitroarenes.[a]

Entry	RC$_6$H$_4$NO$_2$	Time (h)	Yield (%)[b]	TOF (h^{-1})[c]
1	H	1	98	980
2	4-OH	1	96	960
3	2-OH	1.5	95	633
4	4-NH$_2$	1.5	96	640
5	4-CH$_3$	1	96	960
6	4-OCH$_3$	1	92	920
7	4-CN	1	92	420
8	2-NH$_2$	2	90	450
9	4-CHO	2	85	420
10	4-Cl	2	90	450

[a]Reaction conditions: Catalyst (0.1 mol%), nitroarene (1.0 mmol), NaBH$_4$ (2.0 mmol), MeOH:H$_2$O (1:2, 3.0 mL), 60 °C; [b]Isolated yields; [c]TOF, turnover frequencies (TOF = (Yield/Time)/Amount of catalyst (mol).

3.3 Study of reusability

In spite of the excellent catalytic efficiency of the biogenic Au NPs, it is very essential to assess the reusability in view of sustainable catalysis. Therefore, after completion of the fresh batch of probe reaction, the catalyst was retrieved by centrifugation, washed thoroughly with MeOH/H$_2$O mixture, dried and reused in successive cycles. The result has been presented in Fig. 7. Interestingly, the catalyst could be reused up to 12 cycles with almost consistent reactivity.

We compared the outcomes of our developed protocol with the hitherto reported articles in the catalytic reduction of nitrobenzene in order to show the distinctiveness. They have been documented in Table 3. It clearly demonstrates that our method is superior in most over the others.

Table 3. A comparison our protocol with some reported methods for the reduction of nitrobenzene.

Entry	Catalyst	Conditions	Time (h)	Yield (%)	Refs.
1	Fe_3O_4 Ni MNPs	Glycerol, KOH, 80 ºC	3	94	56
2	[Pt]@SiC6	AcOEt, H_2, RT	3	95	57
3	Nickel-iron mixed oxide	$N_2H_4.H_2O$, propan-2-ol, Reflux	1.5	96	58
4	Rh	N_2H_4, EtOH, 80 °C	2.5	99	59
5	Pd Cu/graphene	$NaBH_4$, EtOH:H_2O (1:2), 50 °C	1.5	95	60
6	Fe−phenanthroline/C	$N_2H_4.H_2O$, THF, 100 °C	10	99	61
8	Amberlite-Au NPs	$NaBH_4$, MeOH:H_2O (1:1), 40 ºC	0.33	85	62
8	Au NPs	$NaBH_4$, MeOH:H_2O (1:2), 60 ºC	1	98	This Work

3.4 Anti-human colon cancer potentials of gold nanoparticles

In our study, the treated cells with several concentrations of the present $HAuCl_4$, *Mentha pulegium* extract, and AuNPs were examined by MTT test for 48h regarding the cytotoxicity properties on normal (HUVEC), colorectal adenocarcinoma (HT-29), colorectal carcinoma (HCT 116), ileocecal colorectal adenocarcinoma (HCT-8 [HRT-18]), and Burkitt's lymphoma (Ramos.2G6.4C10) cell lines (Fig. 8; Table 4). The absorbance rate was determined at 570 nm, which indicated extraordinary viability on normal cell line (HUVEC) even up to 1000μg/mL for $HAuCl_4$, *Mentha pulegium* extract, and AuNPs.

In the case of colorectal adenocarcinoma, colorectal carcinoma, ileocecal colorectal adenocarcinoma, and Burkitt's lymphoma cell lines, the viability of them reduced dose-dependently in the presence of $HAuCl_4$, *Mentha pulegium* extract, and AuNPs. The IC50 of *Mentha pulegium* and AuNPs against HT-29 cell line were 421 and 218 μg/mL, respectively; against Human HCT 116 cell line were 380 and 193 μg/mL, respectively; against HCT-8 [HRT-18] cell line was 445 and 269 μg/mL, respectively; and against Ramos.2G6.4C10 cell line were 457 and 285 μg/mL, respectively. The best result of cytotoxicity property of gold nanoparticles against the above cell lines was seen in the case of the HCT 116 cell line.

The anticancer of gold nanoparticles was found to be highly dependent on a range of factors related to their physical characteristics, such as surface coating, shape, and size. About the size, it has been reported that gold nanoparticles with small size can transfer of cell membrane of tumor cells and remove them. In the larger size, the above ability significantly is confined [63]. As can be observed in Figures 3 and 4 of our study, gold nanoparticles had uniform spherical morphology in range sizes of 30-45 nm. The

size of gold nanoparticles in lower than 50 nm is very suitable for the killing of tumor cell lines *in vivo* and *in vitro* [63].

About the anticancer properties of gold nanoparticles, they have used for the treatment of several cancers including human lung cancer, mammary carcinoma, uterus cancer, lung epithelial cancer, Lewis lung carcinoma, colon cancer, and human glioma [64].

Table 4. The IC50 of HAuCl$_4$, *Mentha pulegium,* and AuNPs in the cytotoxicity test.

	HAuCl$_4$ (µg/mL)	*M. pulegium* (µg/mL)	AuNPs (µg/mL)
IC50 against HT-29	-	421	218
IC50 against HCT 116	-	380	193
IC50 against HCT-8 [HRT-18]	-	445	269
IC50 against Ramos.2G6.4C10	-	457	285

4. Conclusion

In conclusion, we herein report the development of a facile green approach for the biogenic synthesis of Au NPs using *Mentha pulegium* flower extract. The phytochemical enriched flora extract has been found to functionalize the Au NPs surface. The synthetic progression of the NPs has been monitored by visible as well as spectroscopic means. Catalytic performance of the biosynthesized Au NPs was investigated in the efficient reduction of several aromatic nitro compounds in presence of NaBH$_4$ as the hydrogen donor under eco-friendly conditions. The amines were obtained in excellent yields with high TOF. Furthermore, the catalyst was proved to be sufficiently robust and truly heterogeneous as it retained its catalytic efficiency up to 12 successive cycles. On the whole, the total protocol described herein could be advantageous for academia as well as industry keeping in view of green and sustainable chemistry. Also, these nanoparticles had effective anti-colon cancer effects against colorectal adenocarcinoma (HT-29), colorectal carcinoma (HCT 116), ileocecal colorectal adenocarcinoma (HCT-8 [HRT-18]), and Burkitt's lymphoma (Ramos.2G6.4C10) cell lines without any cytotoxicity activity against normal cell line i.e., HUVEC. It appears that the gold nanoparticles synthesized using *Mentha pulegium* flower aqueous extract can be used as novel anti-colon cancer drugs in humans in the near future.

Declarations

Ethics approval and consent to participate

Not applicable

Consent for publication

We understand that the information will be published without my/my child or ward's/my relative's (circle as appropriate) name attached, but that full anonymity cannot be guaranteed. We understand that the text and any pictures published in the article will be freely available on the internet and may be seen by the general public. The pictures and text may also appear on other websites or in print, may be translated into other languages or used for commercial purposes.

Availability of data and material

Data availability statements include information on where data supporting the results reported in the article can be found including, where applicable, hyperlinks to publicly archived datasets analyzed or generated during the study.

Competing interests

The authors declare that they have no competing interests.

Funding

Not applicable

Authors' contributions

Maryam Shahriari and Shabnam Bovandi: Visualization, Writing original draft, Formal analysis. M M. Zangeneh: Funding acquisition, Methodology, Supervision, review and editing.

References

1. D.V. Goia, E. Matijevic, *New J. Chem.* **1998**, 22, 1203-1215
2. L. Liu, A. Corma, *Chem. Rev.* **2018**, 118, 4981-5079
3. R. J. Hamers, *Acc. Chem. Res.* **2017**, 50, 633-637
4. J. E. Hutchison, A*CS Sustainable Chem. Eng.* **2016**, 4, 11, 5907-5914
5. P. Gao, W. Pan, N. Li, B. Tang, *ACS Appl. Mater. Interfaces* **2019**, 11, 26529-26558
6. M. Wang, S. K. Mohanty, S. Mahendra, *Acc. Chem. Res.* **2019**, 52, 3, 876-885
7. D. Son, Z. Bao, *ACS Nano* **2018**, 12, 11731-11739
8. N. Naseri, E. Ajorlou, F. Asghari, Y. P-Soltanahmadi, *Artif. Cells, Nanomed., Biotechnol.* **2018**, 46, 1111-1121

9. Q. Zhang, X. Yang, J. Guan, *ACS Appl. Nano Mater.***2019**, 2, 4681-4697

10. M. Hu, Z. Yao, X. Wang, *Ind. Eng. Chem. Res.***2017**, 56, 3477-3502

11. N. Sharma, H. Ojha, A. Bharadwaj, D. P. Pathak, R. K. Sharma, *RSc. Adv.***2015**, **5**, 53381-53403

12. K. Shen, X. Chen, J. Chen, Y. Li, *ACS Catal.***2016**, 6, 5887-5903

13. C. A. Antonyraj, J. Jeong, B. Kim, S. Shin, S. Kim, K. Y. Lee, J. K. Cho, *J. Ind. Eng. Chem.* **2013**, 19 (3), 1056−1059

14. S. Menon, S. Rajeshkumar, S. Venkatkumar, Resource-Efficient Technologies, **2017**, 3, 516−527

15. M. Yazdankhah, H. Veisi, S. Hemmati, *J. Taiwan Inst. Chem. Eng.* **2018**, 91, 38-46.

16. Y. Xia, H. Yang, C. T. Campbell, Acc. Chem. Res. 2013, 46 (8), 1671−1672.

17. P. Anastas, N. Eghbali, *Chem. Soc. Rev.*, **2010**, 39, 301−312

18. P. Anastas, M. M. Kirchhoff, *Acc. Chem. Res.* **2002,** 35, 686-694

19. J. H. Clark, *Acc. Chem. Res.* **2002,** 35, 791-797

20. J. E. Hutchison, *ACS Nano*, **2008**, 2, 395-402

21. R. Varma, *Green Chem.* **2014**, 16, 2027-2041

22. R. Mohammadinejad, S. Karimi, S. Iravani, R. S. Varma, *Green Chem.* **2016**, 18, 20-52

23. S. Machado, S. L. Pinto, J. P. Grosso, H. P. A. Nouws, J. T. Albergaria, C. Delerue-Matos, , *Sci. Total Environ.* **2013,** *445*, 1-8

24. G. Lopez-Tellez, P. Balderas-Hernandez, C. E. Barrera-Diaz, A. R. Vilchis-Nestor, G. Roa-Morales, B. Bilyeu, *J. Nanosci. Nanotechnol.* **2013,** *13*, 2354-2361

25. K. M. Kumar, B. K. Mandal, K. S. Kumar, P. S. Reddy, B. Sreedhar, *Spectrochim. Acta A* **2013,** *102*, 128-133

26. O. V. Kharissova, H. V. R. Dias, B. I. Kharisov, B. O. Pérez, V. M. Pérez, *J. Biotechnol.* **2013**, *31*, 240-248

27. D. Sharma, S. Kanchi, K. Bisetty, *Arab. J. Chem.* **2015**, doi:10.1016/j.arabjc.2015.11.002

28. M. N. Nadagouda, N. Iyanna, J. Lalley, C. Han, D. D. Dionysiou, R. S. Varma, ACS *Sustainable Chem. Eng.* **2014**, 2, 1717−1723

29. M. Sarmah, A. B. Neog, P. K. Boruah, M. R. Das, P. Bharali, U. Bora, *ACS Omega*, **2019**, *4*, 3329-5340

30. P. Vishnukumar, S. Vivekanandhan, S. Muthuramkumar, *ChemBioEng. Rev.* **2017**, *4*, 18-36

31. D. Sun, G. Zhang, X. Jiang, J. Huang, X. Jing, Y. Zheng, J. He, Q. Li, *J. Mater. Chem. A*, **2014**, 2, 1767-1773

32. B. C. Choudhary, D. Paul, T. Gupta, S. R. Tetgure, V. J. Garole, A. U. Borse, D. J. Garole, *J. Environ. Sci.***2017**, 55, 236-246.

33. S. Vimalraj, T. Ashokkumar, S. Saravanan, *Biomed. Pharmacother.* **2018**, 105, 440-448

34. J. Panichikkal, R. Thomas, J. C. John, E. K. Radhakrishnan, *Curr. Microbiol.* **2019**, 76, 503-509

35. M. E. Khan, M. M. Khan, M. H. Cho, *RSC Adv.,***2018**, 8, 13898-13909

36. B. Dong, G. Liu, J. Zhou, A. Wang, J. Wang, R. Jin, H. Lv, *RSC Adv.,***2015**, **5**, 97798-97806

37. A. Annamalai, V. L. P. Christina, D. Sudha, M. Kalpana, P. T. V. Lakshmi, *Colloids Surf. B* **2013**, 108, 60– 65

38. P. Suchomel, L. Kvitek, R. Prucek, A. Panacek, A. Halder, S. Vajda, R. Zboril, *Sci. Rep.* **2018**, 8, 1-11

39. A. Dakshinamoorthy, A. M. Asiri, H. garcia, ACS Catal, **2017**, 7 , 2896-2919

40. R. T. Mertens, S. G. Awuah, *ACS Symposium Series,* **2019**, Vol. 1317, Ch. 2, pp. 19-55

41. A. Wittstock, A. Witchmann, M. Baumer, *ACS Catalysis,* **2012**, 2, 2199-2215

42. A. Corma, H. Garcia, *Chem. Soc. Rev.* **2008**, **37**, 2096-2126

43. K. Layek, M. L. Kantam, M. Shirai, D. N-Hamane, T. Sasaki, H. Maheswaran, *Green Chem.* **2012**, 14, 3164–3174

44. T. Aditya, A. Pal, T. Pal, *Chem. Commun.* **2015**, 51, 9410-9431

45. K. J. Datta, A. K. Rathi, P. Kumar, J. Kaslik, I. Medrik, V. Ranc, R. S. Varma, R. Zboril, M. B. Gawande, *Sci. Rep.* **2017**, *7*, 11585-11596

46. M. M. Ayad, W.A. Amer, M. G. Kotp, *Mol. Catal.* **2017**, *439*, 72-80

47. M. T. Shah, A. Balouch, Sirajuddin, A. A. Pathan, Abdullah, A. M. Mahar, S. Sabir, R. Khattak, A. A. Umar, *Microsyst. Technol.* **2017**, *23*, 5745-5758.

48. Ebrahimie, E., Habashi, A.A., Mohammadie-Dehcheshmeh, M., Ghannadha, M., Ghareyazie, B., Yazdi-Amadi, B. *In Vitro Cell Dev. Biol. Plant* **2006**, *42*, 455–460.

49. (a) Kaneko, K., Katsuhara, T., Kitamura, Y., Nishizawa, M., Chen, Y.P., Hsu, H.Y., *Chem. Pharm. Bull.* **1988**, *36*, 4700–4705; (b) Kitajima, J., Noda, N., Ida, Y., Miyahara, K., Kawasaki, T., *Heterocycles* **1981**, *15*, 791–796.

50. Sajad Badfar-Chaleshtori, Behrouz Shiran, Masoomeh Kohgard, Hassan Mommeni, Akram Hafizi, Mahmood Khodambashi, Neda Mirakhorli, Karim Sorkheh, *Biochemical Systematics and Ecology* **2012**, *42*, 35–48.

51. (a) H. Veisi, M. Ghorbani, S. Hemmati, *Mater Sci Eng C,* **2019**, *98*, 584-593; (b) H. Veisi, S. B. Moradi, A. Saljooqi, P. Safarimehr, *Mater Sci Eng C,* **2019**, 100, 445-452; (c) H. Veisi, T. Tamoradi, B. Karmakar, P. Mohammadi, S. Hemmati, *Mater Sci Eng C,* **2019**, 104, 109919-109927; (d) H. Veisi, L. Mohammadi, S. Hemmati, T. Tamoradi, P. Mohammadi, *ACS Omega,* **2019**, 4, 13991-14003.

52. (a) M. Shahriary, H. Veisi, M. Hekmati, S. Hemmati, *Mater Sci Eng C,* **2018**, 90, 57-66; (b) H. Veisi, T. Ozturk, B. Karmakar, T. Tamoradi, S. Hemmati, Carbohydrate Polymers 235 (2020) 115966; (c) H. Veisi, A. Mirzaei, P. Mohammadi, RSC Adv., 9 (2019) 41581; (d) H. Veisi, T. Tamoradi, B. Karmakar, S. Hemmati, J. Phys. Chem. Solids 138 (2020) 109256; (e) H. Veisi, P. Mohammadi, T. Ozturk, J. Molecular Liquids 303 (2020) 112625; (f) G. Shaham, H. Veisi, M. Hekmati, Appl Organometal Chem. 31 (2017) e3737; (j) H. Veisi, Y. Metghalchi, M. Hekmati, S. Samadzadeh, Appl Organometal Chem. 2017, 31, e3676.

53. (a) M. M. Zangeneh, A. Zangeneh, E. Pirabbasi, R. Moradi, M. Almasi. Appl Organometal Chem. 33 (2019) e5246. DOI: 10.1002/aoc.5246. (b) B. Mahdavi, S. Paydarfard, M. M. Zangeneh, S. Goorani, N. Seydi, A. Zangeneh. Appl Organometal Chem. 33 (2019) e5248. DOI:10.1002/aoc.5248. (c) A. R.

Jalalvand, M. Zhaleh, S. Goorani, M. M. Zangeneh, N. Seydi, A. Zangeneh, R. Moradi, J Photochem Photobiol B. 192 (2019) 103−112. (d) M. Zhaleh, A. Zangeneh, S. Goorani, N. Seydi, M.M. Zangeneh, R. Tahvilian, E. Pirabbasi, *Appl Organometal Chem*. 33 (2019) e5015. (e) M. Shahriari, S. Hemmati, A. Zangeneh, M.M. Zangeneh, Appl Organometal Chem. 33 (2019) e5189. DOI: 10.1002/aoc.5189. (f) M.M. Zangeneh, S. Saneei, A. Zangeneh, R. Toushmalani, A. Haddadi, M. Almasi, A. Amiri-Paryan, Appl Organometal Chem. 33 (2019) e5216. DOI: 10.1002/aoc.5216. (g) S. Goorani, M.K. Koohi, H. Morovvati, J. Hassan, A. Ahmeda, M.M. Zangeneh. Appl. Organometal. Chem. 34 (2020) e5465. (h) Zangeneh A, Zangeneh MM. Appl Organometal Chem 33 (2019) e5290. DOI:10.1002/aoc.5290. (i) S. Hemmati, Z. Joshani, A. Zangeneh, M.M. Zangeneh, Appl. Organometal. Chem. 34 (2020) e5267. DOI:10.1002/aoc.5267.

54. A.K. Abay, X. Chen, D.H. Kuo, New J. Chem. 41 (2017) 5628−5638.

55. G. Wu, X. Liu, P. Zhou, L. Wang, M. Hegazy, X. Huang,Y. Huang, Mat. Sci. Eng. C. 94 (2019) 524−533.

56. M. B. Gawande, A. K. Rathi, P. S. Branco, I. D. Nogueira, A. Velhinho, J. J. Shrikhande, U. U. Indulkar, R. V. Jayaram, C. A. A. Ghumman, N. Bundaleski, O. M. N. D. Teodoro, *Chem. Eur. J.* , **2012**, *18*, 12628-12632

57. Y. Motoyama, K. Kamo, H. Nagash, *Org. Lett*. **2009**, *11*, 1345-1348

58. Q. Shi, R. Lu, L. Lu, X. Fu, D. Zhao, *Adv. Synth. Catal*. **2007**, *349*, 1877-1881

59. M. Shokouhimehr, J. E. Lee, S. I. Han, T. Hyeon, *Chem. Commun*. **2013**, *49*, 4779-4781

60. Y.-S. Feng, J.-J. Ma, Y.-M. Kang, H.-J. Xu, *Tetrahedron***2014**, *70*, 6100-6105

61. R. V. Jagadeesh, G. Wienhofer, F. A. Westerhaus, A.-E. Surkus, M.-M. Pohl, H. Junge, K. Junge, M. Beller, *Chem. Commun*., **2011**, *47*, 10972-10974.

62. D. Shah, H. Kaur, J. Mol. Catal. A Chem. 381 (2014) 70− 76.

63. (a) S. Hemmati, Z. Joshani, A. Zangeneh, M.M. Zangeneh, *Appl Organometal Chem.* **2019**, *33*, e5277. DOI:10.1002/aoc.5277. (b) S. Hemmati, P. Irani, A. Zangeneh, M.M. Zangeneh, *Appl Organometal Chem.* **2019**, *33*, e5274. DOI:10.1002/aoc.5274. (c) M.M. Zangeneh, *Appl Organometal Chem.* **2019**, *33*, e5295. DOI:10.1002/aoc.5295. (d) G. Mohammadi, M.M. Zangeneh, A. Zangeneh, Z.M. Siavosh Haghighi, *Appl Organometal Chem.* **2019**, *33*, e5136. DOI:10.1002/aoc.5136. (e) M. M. Zangeneh, S. Bovandi, S. Gharehyakheh, A. Zangeneh, P. Irani, *Appl Organometal Chem.***2019**, *33*, e4961. (f) M. Hamelian, M.M. Zangeneh, A. Shahmohammadi, K. Varmira, H. Veisi, *Appl Organometal Chem.* **2019**, *33*, e5278. DOI:10.1002/aoc.5278. (g) S. Hemmati, A. Rashtiani, M. M. Zangeneh, P. Mohammadi, A. Zangeneh, H. Veisi, *Polyhedron.* **2019**, *158*, 8−14. (h) M. M. Zangeneh, Z. Joshani, A. Zangeneh, E. Miri, *Appl Organometal Chem.***2019**, *33*, e5016. (i) A. Zangeneh, M. M. Zangeneh, R. Moradi. *Appl Organometal Chem.* **2019**, *33*, e5247. DOI:10.1002/aoc.5247.

64. P. Singh, S. Pandit, V. R. S. S. Mokkapati, A. Garg, V. Ravikumar, I. Mijakovic, *Int J Mol Sci.* **2018**, *19*, 1979.
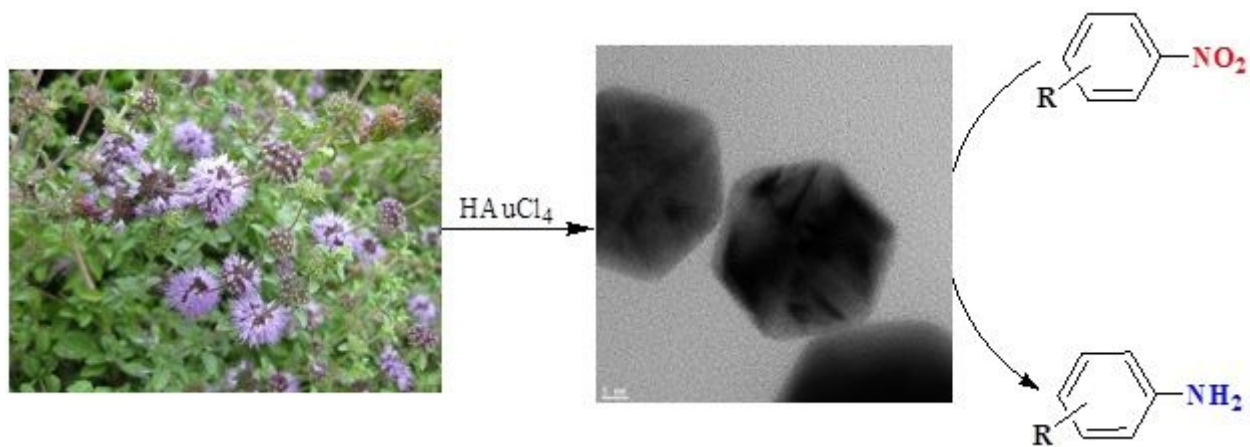
Figures

Figure 1

Synthetic procedure towards biogenic Au NPs and its application in the reduction of nitroarenes in water.
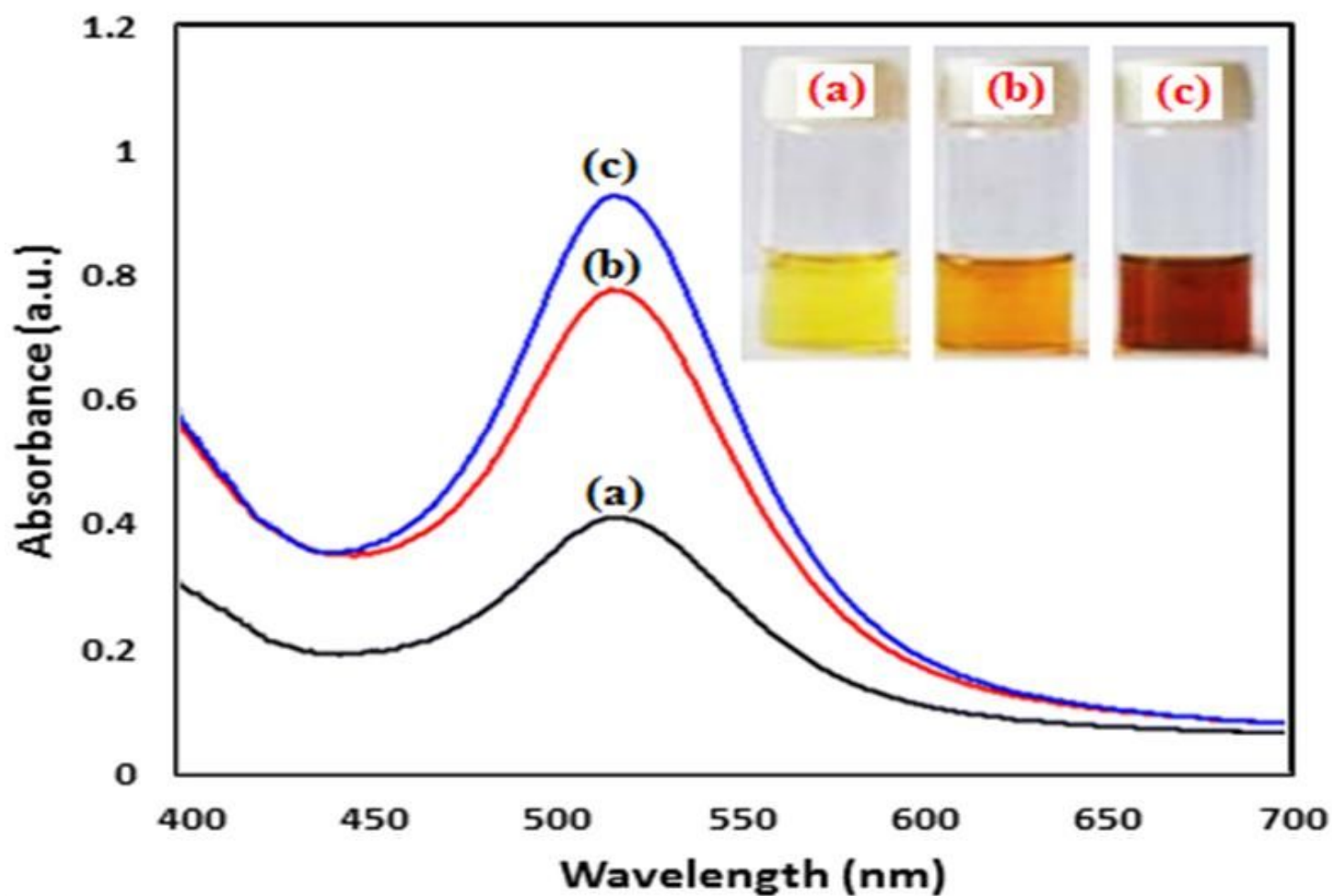

Figure 2

UV-Vis spectra and corresponding color changes with time during the biosynthesis of Au NPs.
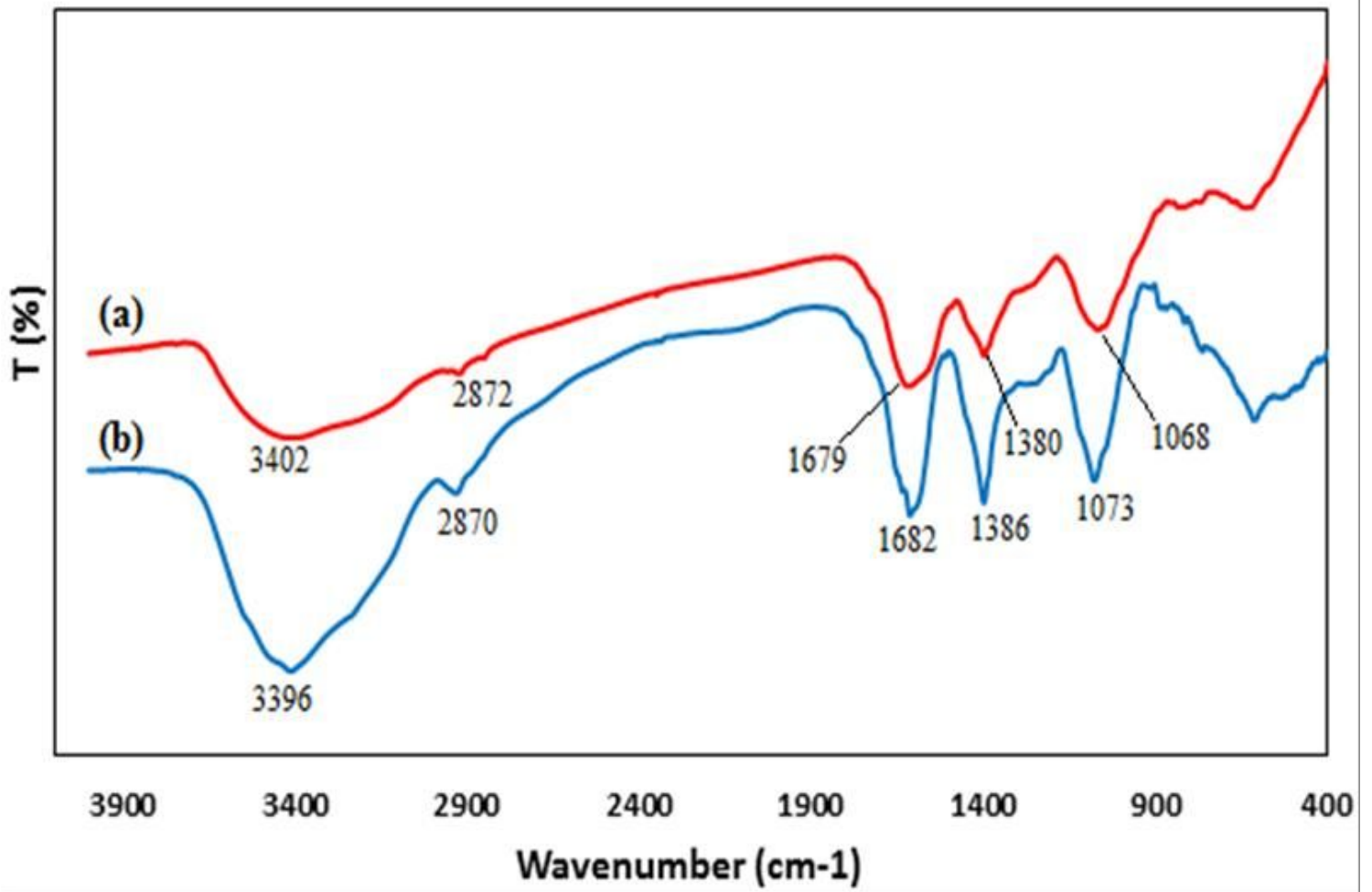
Figure 3

FT-IR spectra of (a) Mentha pulegium extract and (b) biosynthesized Au NPs.
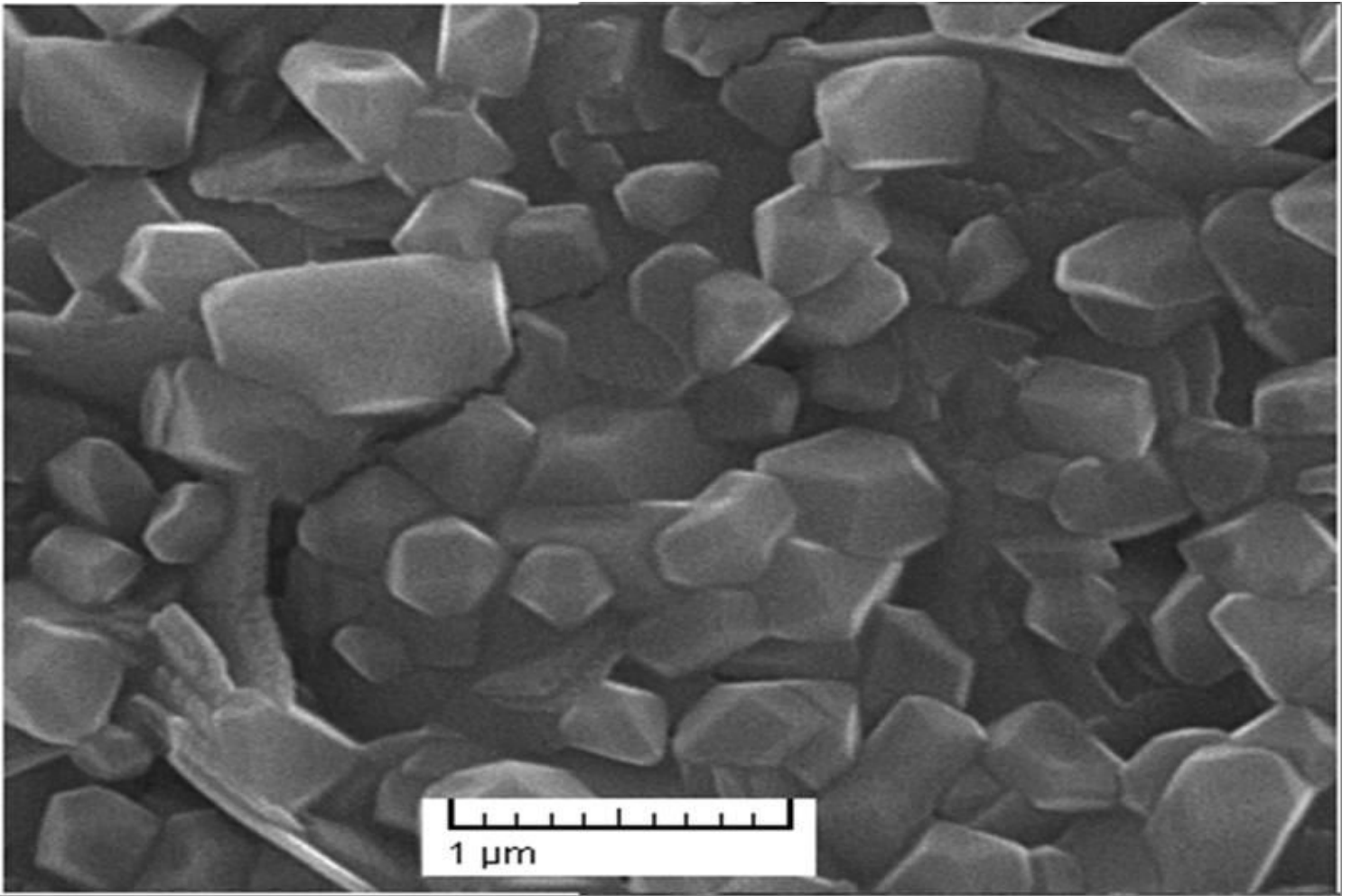
Figure 4

FT-IR spectra of (a) Mentha pulegium extract and (b) biosynthesized Au NPs.
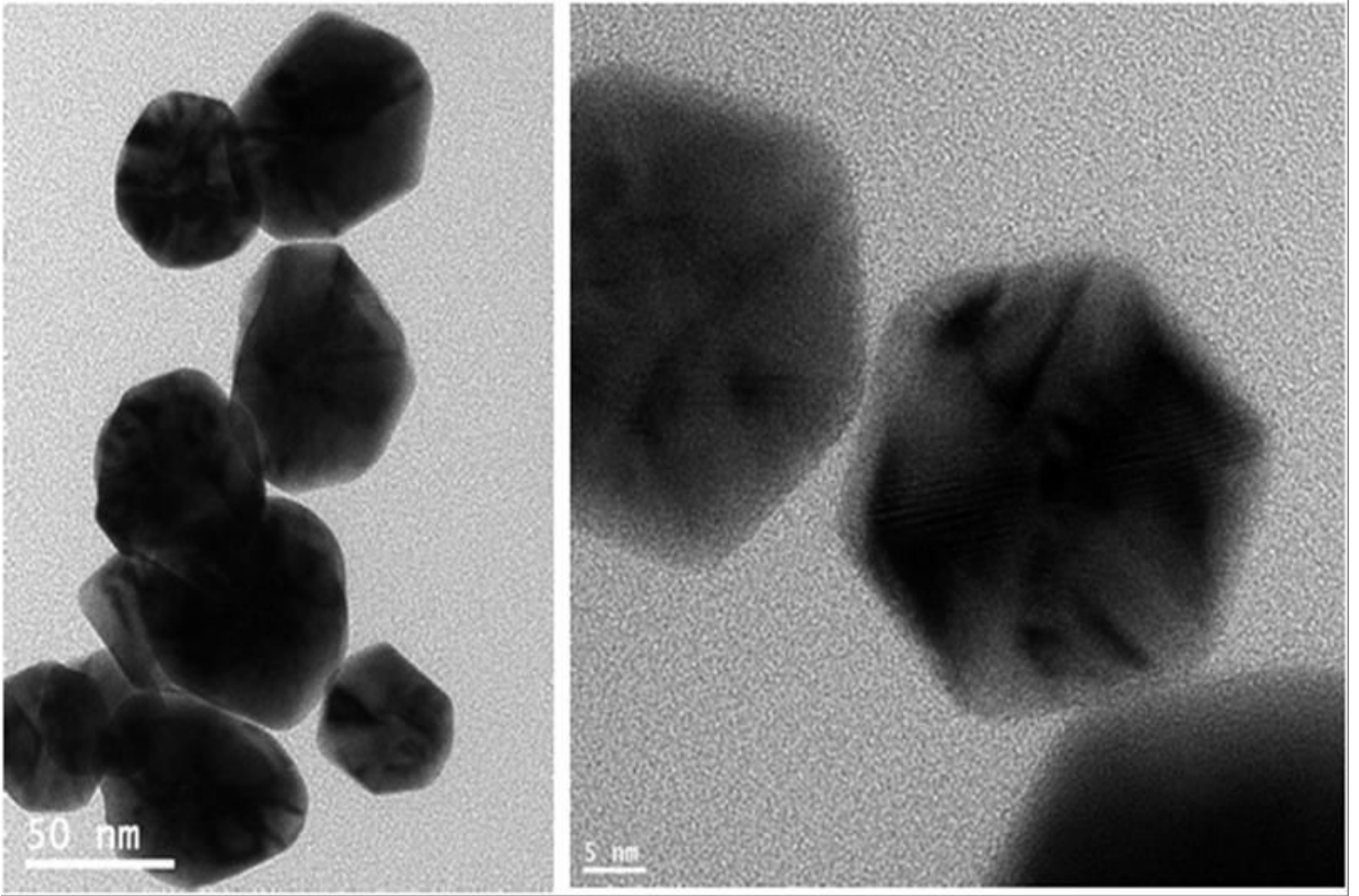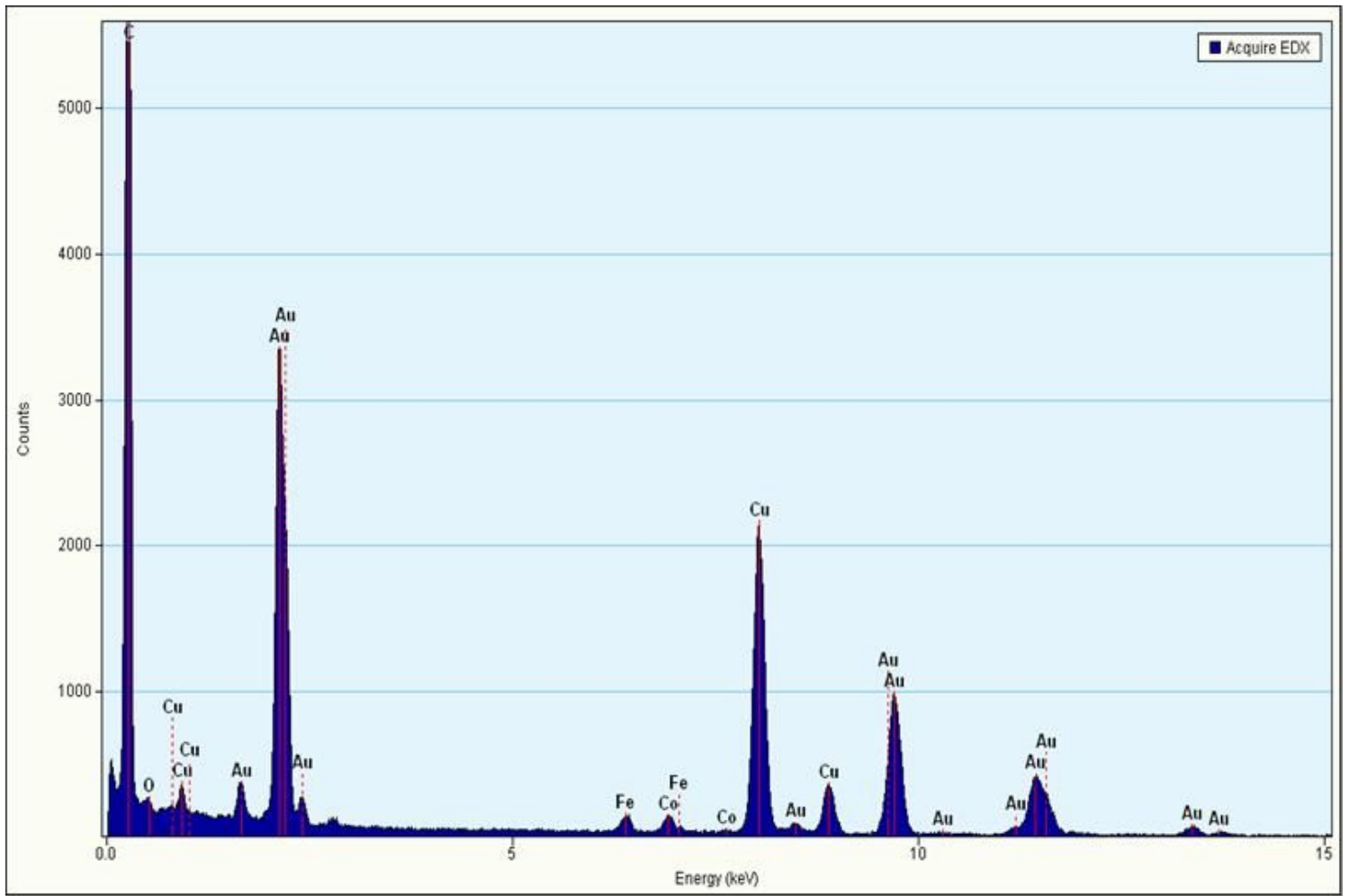
Figure 5

HR-TEM images of biosynthesized Au NPs.

Figure 6
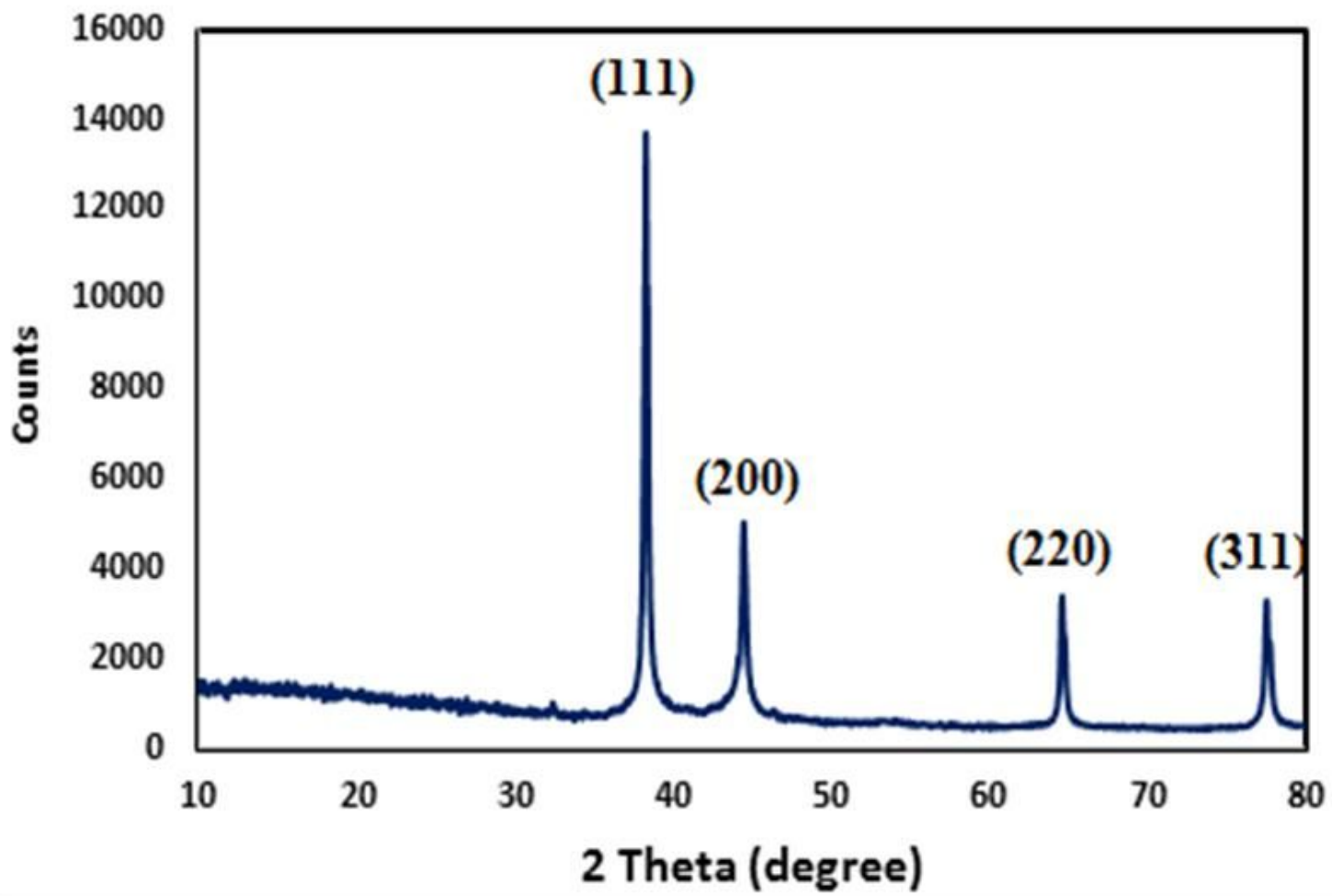
EDX spectrum of biosynthesized Au NPs.

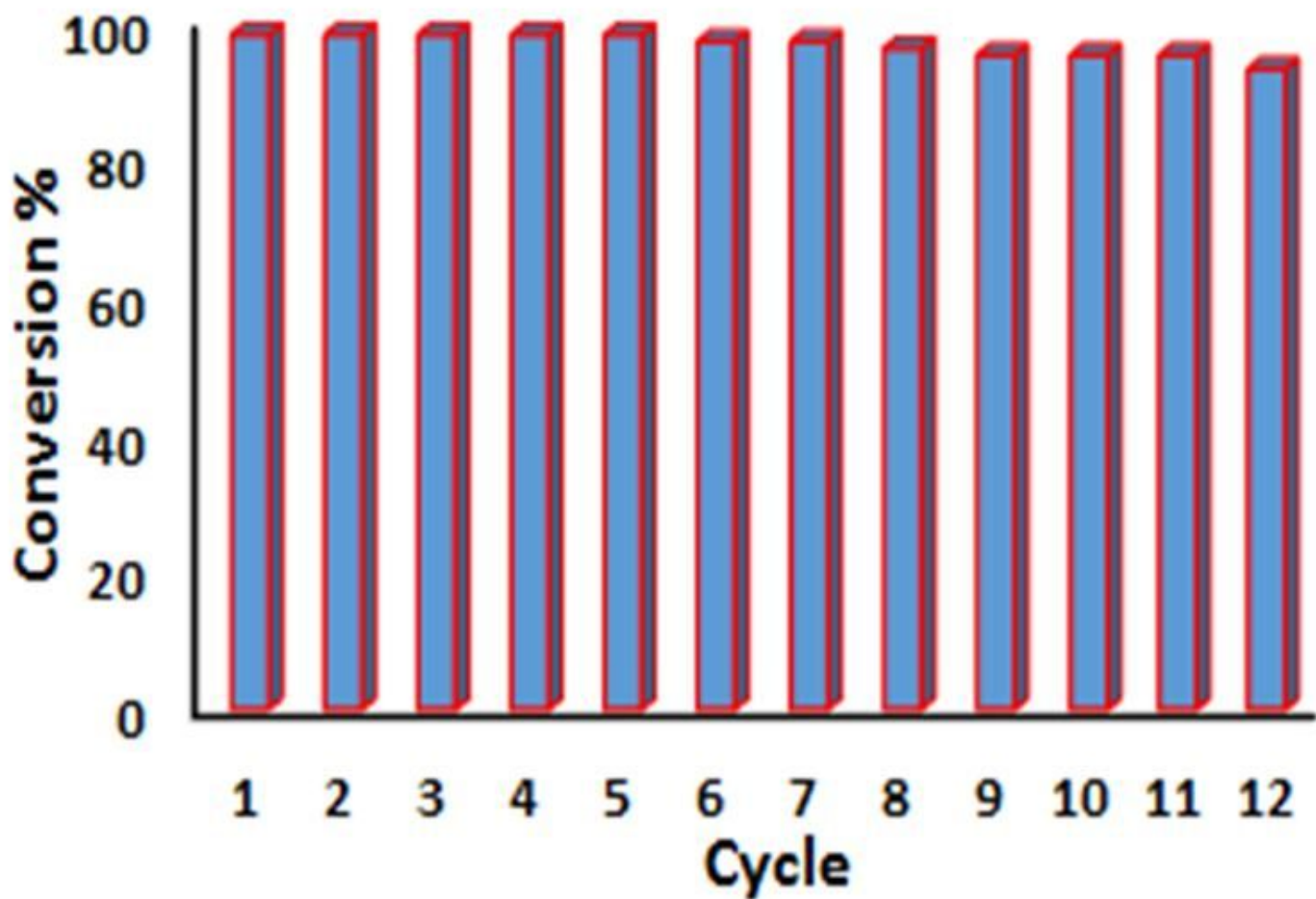**Figure 7**

XRD pattern of biosynthesized Au NPs.

Figure 8

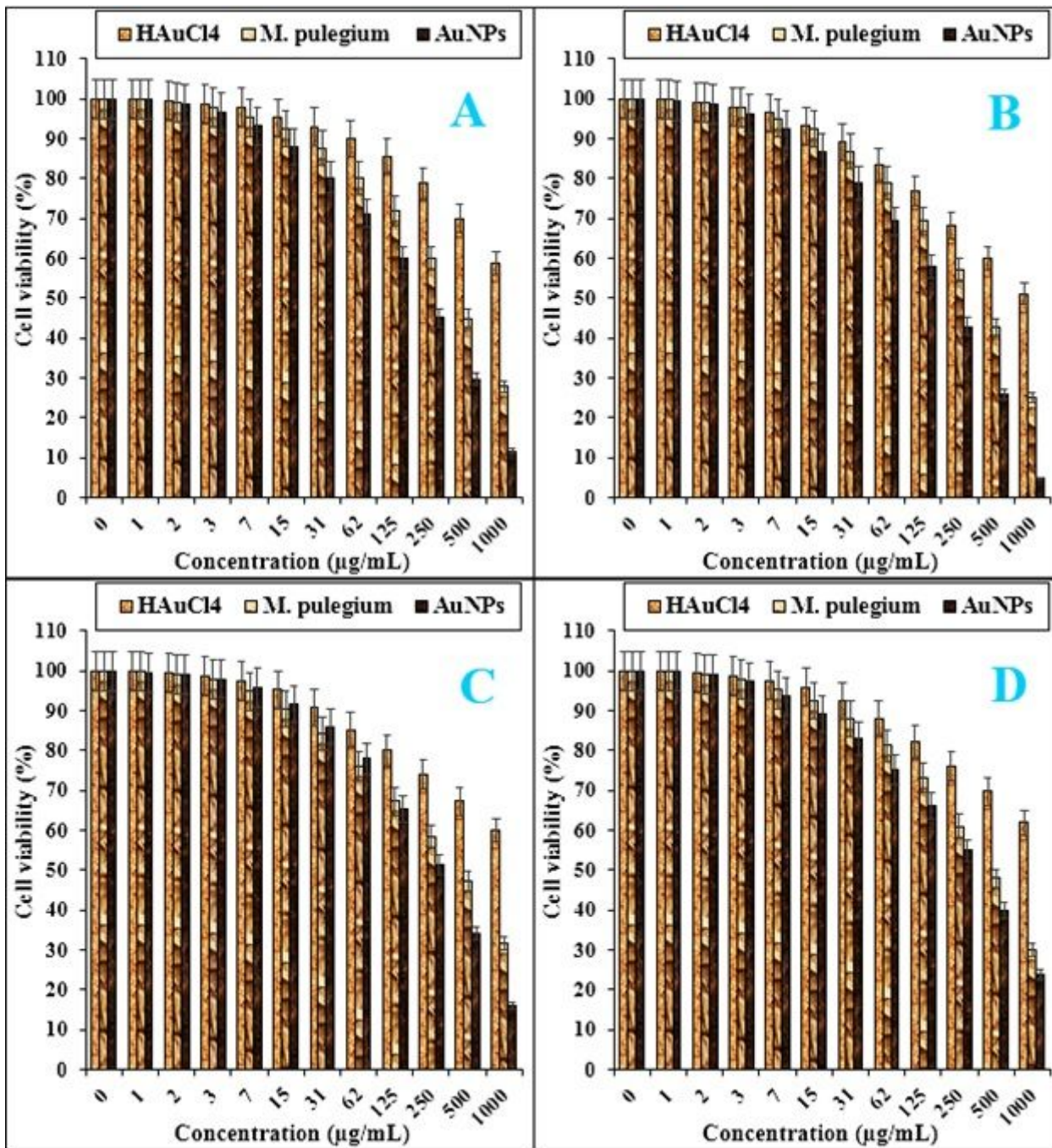Reusability of biosynthesized Au NPs for reduction of nitrobenzene.

Figure 9

The anti-colorectal carcinoma properties of HAuCl4, Mentha pulegium, and Au NPs against HT-29 (A), HCT 116 (B), HCT-8 [HRT-18] (C), and Ramos.2G6.4C10 (D) cell lines.